Cellulose nanofiber aerogels impregnated with bio-based epoxy using vacuum infusion: structure, orientation and mechanical properties

Tuukka Nissilä [a], Sakari S. Karhula [b, c], Simo Saarakkala [b, d, e], Kristiina Oksman [a, f, *]

[a] Fibre and Particle Engineering Research Unit, Faculty of Technology, University of Oulu, FI-90014 Oulu, Finland

[b] Research Unit of Medical Imaging, Physics and Technology, University of Oulu, FI-90014 Oulu, Finland

[c] Infotech, Univesity of Oulu, FI-90014 Oulu, Finland

[d] Medical Research Center, University of Oulu, FI-90014 Oulu, Finland

[e] Department of Diagnostic Radiology, Oulu University Hospital, Oulu, Finland

[f] Division of materials science, Department of Engineering Sciences and Mathematics, Luleå University of Technology, SE-97187 Luleå, Sweden

* Corresponding author. E-mail address: kristiina.oksman@ltu.se (K. Oksman).

Abstract: Cellulose nanofiber aerogels were used as preforms that were impregnated with a bio-epoxy resin via a widely used vacuum infusion process. The simple and straightforward nanocomposite processing approach resulted in an almost 70 % improvement in the storage modulus of the polymer with only an 11.7 wt% cellulose nanofiber content. The nanofibers were well dispersed in the polymer matrix and the fiber structures were anisotropically aligned. The impregnation time of the aerogels was also significantly lower than that of the more commonly used nanopapers. It was thus shown that environmentally friendly and mechanically robust nanocomposites could be produced by impregnating cellulose nanofiber aerogels with a thermosetting resin, using a processing approach that has a potential to be scaled up for commercial use.

Keywords: Nano composites, Mechanical properties, Anisotropy, Aerogels

1 Introduction

To reduce our dependence on non-renewable resources in composites manufacture, the more commonly used reinforcement materials, such as carbon and glass fibers, should be replaced with renewable alternatives. One promising reinforcement material for such composites is cellulose nanofibers (CNFs). They have good mechanical properties, a relatively low density, and are widely available and renewable [1]. However, even after over 20 years of research, the critical steps of dispersing CNFs in a hydrophobic polymer and controlling the resulting fiber structure are still major issues.

To overcome the problem of dispersion, the strong network-forming tendency of CNFs has been widely utilized by preparing nanofiber networks, also called nanopapers, and impregnating them with a polymer. Using impregnation methods with thermosetting resins is a potential way of producing strong and stiff composite materials [2,3]. A good fiber dispersion can be achieved because the polymer is introduced into the rigid and fixed network structure instead of directly mixing the individual fibers and the matrix. However, the process may take up to several days to complete and solvents have to be used to decrease the viscosity of the polymer. Solvents can also be used to increase the porosity of the network and to facilitate the impregnation process [4,5] but these procedures are usually complicated and the resulting networks may still be very difficult to impregnate. In addition, in these kind of networks the fibers are randomly oriented. The strength of cellulose nanocomposites is found to rely heavily on the properties of the network [6], suggesting that controlling the fiber structure is a critical step in preparing composites with desirable properties. Various methods such as wet stretching [7,8], dry spinning [9,10], wet spinning [11,12] and hydrodynamic alignment [13] can be utilized to anisotropically orient CNFs and to improve the properties, but the

resulting materials are either thread-like single filaments or thin paper-like sheets that are not readily compatible with structural applications.

Freeze casting is a promising method to obtain CNF network structures that are both highly porous and oriented [14–16]. This method results in a dry, self-standing CNF network, also commonly called aerogel. Attempts at impregnating CNF aerogels with a resin to obtain composites include filling a polyvinyl alcohol (PVA)/CNF hybrid aerogel with polydimethylsiloxane (PDMS) [17] and filling an aerogel prepared from TEMPO-treated CNFs with bio-based epoxy [18]. In both cases, silylating the aerogels before impregnation played an important role in improving the filling with the hydrophobic polymer. However, the fiber content in the resulting composites was very low, making the mechanical properties quite modest.

To obtain a strong and stiff composite with a well-dispersed and oriented fiber structure, we impregnated a CNF aerogel with a bio-epoxy resin. Vacuum infusion was used to reduce the filling time and to increase the fiber content of the composite. This paper presents the straightforward method of preparing aerogels via freeze casting and using them as anisotropically oriented preforms in a commercially applicable vacuum infusion process to produce nanocomposites. The structure and properties of both the aerogels and the composites are also discussed along with suggestions for future studies.

2 Experimental

2.1 Materials

Bleached softwood kraft pulp (90 % pine, 10 % spruce, Stora Enso, Oulu, Finland) was used as a CNF source. 120 g (dry weight) of cellulose was mechanically fibrillated by grinding (Super Masscolloider MKCA 6-2J CE, Masuko Sangyo Co, Ltd., Kawaguchi, Japan) a 1.6 wt% suspension for approximately 210 minutes to obtain an

aqueous CNF gel. The gap between the grinding stones was gradually adjusted to -90 µm. The diameters of the resulting fibers ranged from a few nanometers to tens of micrometers (Fig. 1). To prepare aerogels with different fiber contents the initial CNF suspension was either diluted with deionized water or concentrated by centrifugation and subsequent dilution. All suspensions were mixed and degassed in a planetary mixer (THINKY ARE-250, Thinky Corp., Tokyo, Japan) for 3 + 3 minutes (mixing + degassing) prior to the freeze casting process.

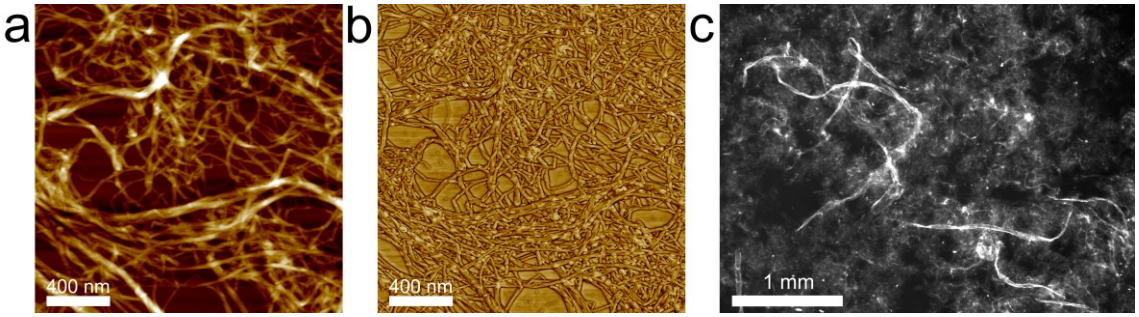

Fig. 1. CNF morphology. AFM (a) height and (b) phase images and (c) an optical microscope image showing the various fiber sizes present in the material.

The polymer matrix used in the composite preparation was an optically brightened bio-epoxy resin (SUPER SAP® BRT, Entropy Resins, Hayward, USA) with a 21 % bio-based carbon content. The resin contains renewable materials for example from waste streams of wood pulp and bio-fuels production. Two different hardeners (SUPER SAP® CLX and INH, Entropy Resins, Hayward, USA) were mixed with a 100:3:29 (BRT:CLX:INH) mixing ratio (by weight). According to the manufacturer's data sheet, the initial room temperature viscosity of the mixture was approximately 200 mPas and the pot life was over 180 minutes.

2.2 Sample preparation

The porous CNF preforms, or aerogels, were prepared via freeze casting. A CNF suspension with 1, 3 or 5 wt% fiber content was frozen in a polytetrafluoroethylene

(PTFE) mould using a dry ice-acetone cooling bath. The copper bottom plate of the mould was kept immersed in the freezing medium (-78 °C) until the sample was completely frozen. The mould with the frozen suspension was put in a freeze dryer (-53 °C and 0.05 mbar) for 24-96 hours, depending on the sample size. Three different mould shapes were used to obtain aerogels with varying dimensions.

Nanocomposite was prepared by impregnating a 65 mm high 1 wt% CNF aerogel with a bio-epoxy resin via vacuum infusion (Fig. 2). The CNF preform and sheets of porous distribution medium were placed on a metal plate and covered with a sealed plastic film. Two tubes, an inlet and an outlet, were attached to the system and a vacuum pressure of approximately 35 mbar was applied to the outlet tube. When no leaking of air was observed, the inlet tube immersed in a premixed and degassed resin/hardener mixture was unclamped to start the resin flow into the system. The infusion occurred primarily along the aerogel freezing direction and continued at room temperature for approximately 1.5 hours. After the infusion, both the inlet and the outlet tubes were clamped and the sample was left to cure under vacuum for 24 hours. Before clamping the tubes, weight was applied on the sample to decrease the thickness variation along the sample length. After 24 hours, the sample was demoulded and post cured at 50 °C for 16 hours. A neat epoxy control sample was prepared by pouring a small amount of the epoxy/hardener mixture on a Petri dish and curing it for 24 hours at room temperature and for 16 hours at 50 °C.

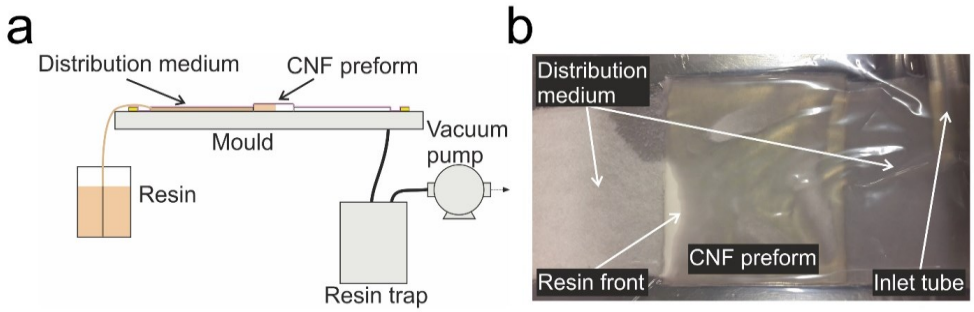

Fig. 2. The vacuum infusion process. (a) A schematic illustration and (b) a photograph of the used vacuum infusion setup.

2.3 Aerogel porosity and composite fiber content

The porosity of the aerogels was calculated by measuring the weight and dimensions of the sample and using the density thus obtained to calculate the porosity as

$$\varphi_{aerogel} = \left(1 - \frac{\rho_{aerogel}}{\rho_{CNF}}\right) * 100\ \%, \quad (1)$$

where $\varphi_{aerogel}$ is the porosity of the aerogel, $\rho_{aerogel}$ is the density of the aerogel and ρ_{CNF} is the density of cellulose nanofibers. The sample volumes were estimated by measuring the dimensions with a digital caliper. The weighing was performed immediately after the samples had been removed from the freeze dryer. A cellulose nanofiber density of 1.5 g/cm^3 was used in the calculations [3].

The fiber weight fraction in the composite sample was calculated by dividing the weight of the aerogel before impregnation by the final weight of the composite after curing. The volume fraction of the fibers was calculated as

$$V_f = \frac{v_f}{v_c} = \frac{{}^{m_f}/_{\rho_f}}{v_c}, \quad (2)$$

where V_f is the fiber volume fraction, v_f is the volume of the fibers, v_c is the volume of the composite sample, m_f is the mass of the fibers (mass of the aerogel) and ρ_f is the density of the fibers. The volume of the composite was estimated by measuring the

dimensions with a digital caliper and a precision gauge. The mass of the matrix phase was taken as the difference between the mass of the composite and the mass of the aerogel and the matrix volume fraction V_m was calculated similarly to V_f. The density of the polymer matrix was measured with an automatic gas pycnometer (AccuPyc II 1340, Micromeritics, Norcross, USA). The rest of the volume was assumed to be void.

2.4 Characterization

The morphology of the CNFs was studied with an optical microscope (Leica MZ FL III, Leica Camera AG, Wetzlar, Germany) and an atomic force microscope (AFM) (MultiMode scanning probe, Veeco, Santa Barbara, USA). The AFM samples were prepared by applying a drop of CNF suspension on a mica sheet attached to a sample holder and drying in a vacuum oven. Tapping mode in air was used for the analyses.

Field emission scanning electron microscope (FE-SEM) was used to study the microstructure of the CNF aerogels (ZEISS Sigma HD VP FE-SEM, Carl Zeiss AG, Oberkochen, Germany) and the composite sample (ZEISS ULTRA plus FE-SEM, Carl Zeiss AG, Oberkochen, Germany). A 5 kV acceleration voltage was used. Small aerogel and composite specimens were prepared for imaging by fracturing the samples. The specimens were sputter coated with platinum to avoid charging.

Micro-computed tomography (micro-CT) was used to obtain 3-dimensional reconstructions of the aerogel and composite structures. The specimens were attached to sample holders with a superglue and imaged with a Skyscan 1272 micro-CT system (Bruker microCT, Kontich, Belgium) using the following parameters: 40 kV tube voltage, 250 μA tube current, 3600 projections, 1000 ms exposure time, averaging 4 frames/projection, and 0.8 μm isotropic voxel size. For the imaging of the composite, the number of averaged frames was increased to 8 to increase the signal-to-noise-ratio.

The projections were reconstructed with NRecon-software (v.1.6.9.8, Brüker microCT, Kontich, Belgium). Ring artifact and beam hardening corrections were applied during the reconstruction procedure. The 3D volumes of aerogels were rendered with CTVox (v. 3.3.0 r1403, Brüker microCT, Kontich, Belgium). The 3D model of the composite was generated with CTAnalyser (v. 1.16.4.1, Brüker microCT, Kontich, Belgium).

The compressive strengths of the aerogels were measured with a dynamic mechanical analyzer (Q800 DMA, TA Instruments, New Castle, USA) equipped with an 18 N load cell. The test specimens were 5 x 5 x 5 mm^3 cubes cut from the center part of the approximately 65 mm high samples. The testing was conducted at room temperature with a 2 N/min compression rate, a maximum load of 18 N and a preload of 0.05 N. The samples were tested in both the longitudinal and the transverse directions, that is, the directions parallel and perpendicular to the freezing direction, respectively. Average results of at least six measurements are reported.

The specific surface area of the aerogels was determined with an automated ASAP 2020 (Micromeritics, Norcross, USA) system using N_2 physisorption. The samples were dried in an oven at 105 °C for 18 hours prior to the analysis.

The viscoelastic properties of both the composite and the neat epoxy samples were characterized with dynamic mechanical analysis (Q800 DMA, TA Instruments, New Castle, USA). The testing was conducted under three point bending mode with a constant frequency of 1 Hz and a temperature ranging from 30 to 200 °C. The temperature was increased at a constant rate of 3 °C/min. Rectangular specimens with dimensions of 25 x 3 x 1.0-1.4 mm^3 (l x w x t) were cut for the testing. Gauge length was set at 20 mm. At least two specimens were tested for each condition. The composite sample was tested in both the longitudinal and the transverse directions.

3 Results and discussion

3.1 Aerogel structure and morphology

The aerogels prepared from a 1 wt% CNF suspension were soft and elastic, while the 3 and 5 wt% suspensions resulted in more rigid samples. All the aerogels were surprisingly strong and endured moderate bending, compression and stretching (Fig. 3). The densities and porosities of the samples varied depending on the CNF concentration in the initial suspension but the specific surface area did not change significantly as seen in Table 1.

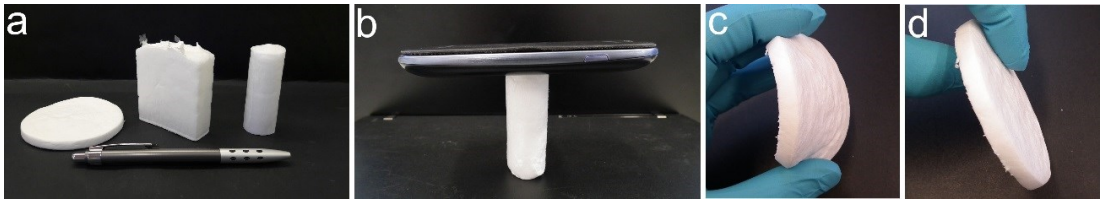

Fig. 3. Photographs of aerogels. (a) Three differently shaped samples (in all of the samples the freezing direction is from bottom up), (b) a sample supporting ~400 times its weight and a sample (c) being bent and (d) after bending.

Table 1. Density, porosity and BET specific surface area of the prepared aerogels.

CNF concentration (wt%)	Density (kg/m^3)	Porosity (%)	BET specific surface area (m^2/g)
1	9	99.4	10.4 ± 4.0
3	29	98.0	9.9 ± 1.2
5	43	97.1	9.0 ± 0.1

Cellular and lamellar fiber structures that are aligned along the freezing direction can be seen in the FE-SEM images showing vertical fracture surfaces of 1 wt% aerogels (Fig. 4 a-d, see also Supplementary data). They have been formed as the growing ice

crystals have arranged the CNFs and the ice has been sublimated to leave open channels between the pore walls. The size of the pores increases as the distance from the bottom of the mould increases, as seen in Fig. 4 a-c showing the bottom, middle and top parts of an approximately 65 mm high aerogel. The phenomenon is a consequence of the increasing thermal resistance between the suspension and the freezing source. The freezing rate directly affects the structure wavelength λ, that is, the pore size. The relation can be described with a power law, $\lambda \propto v^{-n}$, where n has been suggested to depend on the particle size and concentration [19,20].

Higher CNF concentrations resulted in denser structures with smaller pores that are not so well defined (Fig. 4 e, f). The structures are not as distinct or clearly oriented along the freezing direction as in the 1 wt% sample. The fibers also appear to be more aggregated. The presence of large fiber aggregates and an increased amount of fiber-fiber interaction may interfere with the freezing process in such a way that the ice crystals grow tilted or the particles get trapped inside the advancing ice front, leading to an isotropic structure [19]. This is confirmed by the images of 3-dimensional reconstructions based on micro-CT scanning (Fig. 5). The side view of the 1 wt% sample (Fig. 5 a) shows clear orientation along the freezing (vertical) direction and channels can be seen within the aerogel. In the 3 wt% sample (Fig. 5 b) the orientation is not so distinct and the 5 wt% sample (Fig. 5 c) appears to have an isotropic structure. The top views of the 1 and 3 wt% samples (Figure 5 d, e) in turn show clear tubular structures that are not present in the 5 wt% sample (Fig. 5 f).

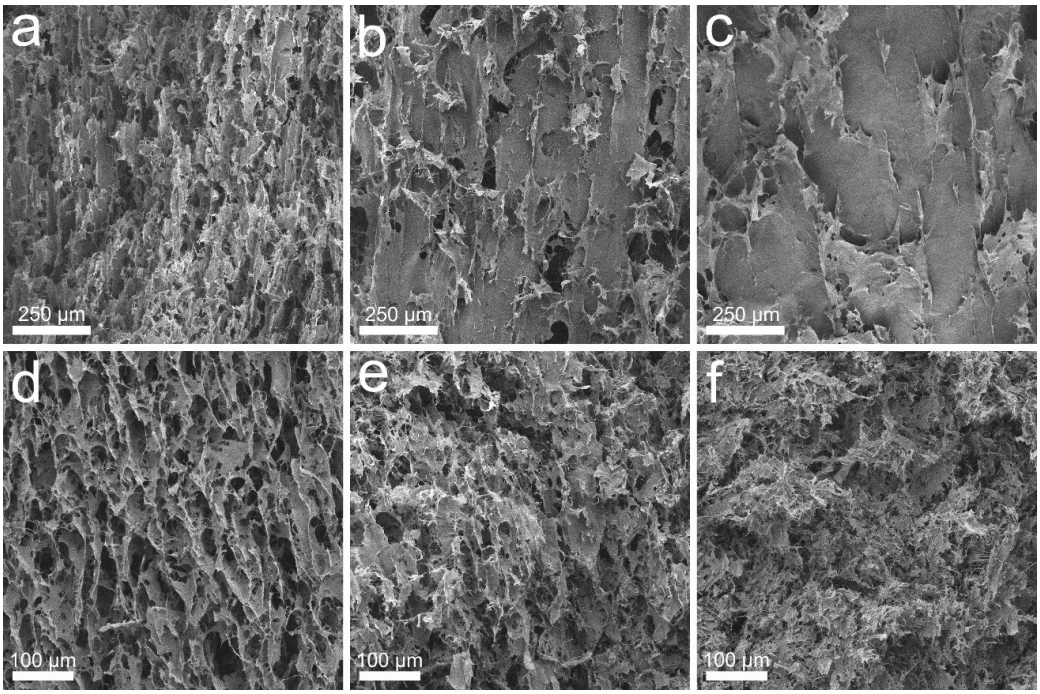

Fig. 4. Microstructure of the CNF aerogels. FE-SEM images of fractured vertical cross sections of the (a) bottom, (b) middle and (c) top parts of an ~65 mm high 1 wt% sample, and of middle parts of ~9 mm high (d) 1 wt%, (e) 3 wt% and (f) 5 wt% samples.

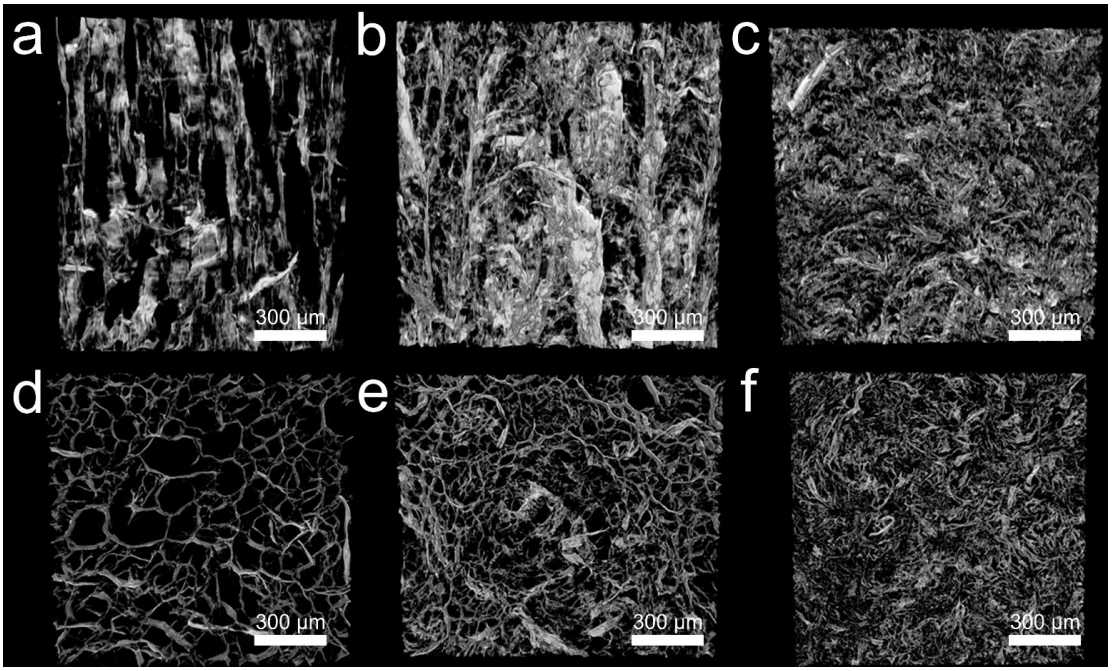

Fig. 5. Images of 3D micro-CT reconstructions of the aerogels. (a-c) Vertical and (d-f) horizontal cross-sections of 1 wt% (a, d), 3 wt% (b, e) and 5 wt% (c, f) aerogels.

3.2 Aerogel compressive strength

Results of the compression tests show anisotropic mechanical properties in the lower concentration aerogels. Especially the samples prepared from a 1 wt% CNF suspension have a significantly higher strength in the longitudinal direction than in the transverse direction (Table 2, Fig. 6). This is an indication of a unidirectional alignment of the CNF structures. The longitudinal direction represents the direction parallel to the freezing direction during the freeze casting process and is thus the direction along which most of the nanofiber structures are aligned. The difference between the compressive strengths measured in the two directions is smaller in the 3 wt% samples and in the 5 wt% samples the properties appear almost isotropic, further confirming the observations made in the previous section.

Table 2. Aerogel compressive strengths. The testing was conducted in both the longitudinal (∥) and the transverse (⊥) directions.

Aerogel sample	Stress at 20 % strain (kPa)	Stress at 40 % strain (kPa)
1 wt% (∥)	16.5 (± 1.1)	20.9 (± 1.2)
1 wt% (⊥)	3.9 (± 0.5)	7.5 (± 0.6)
3 wt% (∥)	78.3 (± 9.8)	124 (± 13)
3 wt% (⊥)	55.4 (± 5.4)	82.4 (± 6.7)
5 wt% (∥)	116 (± 15)	222 (± 27)
5 wt% (⊥)	164 (± 32)	261 (± 43)

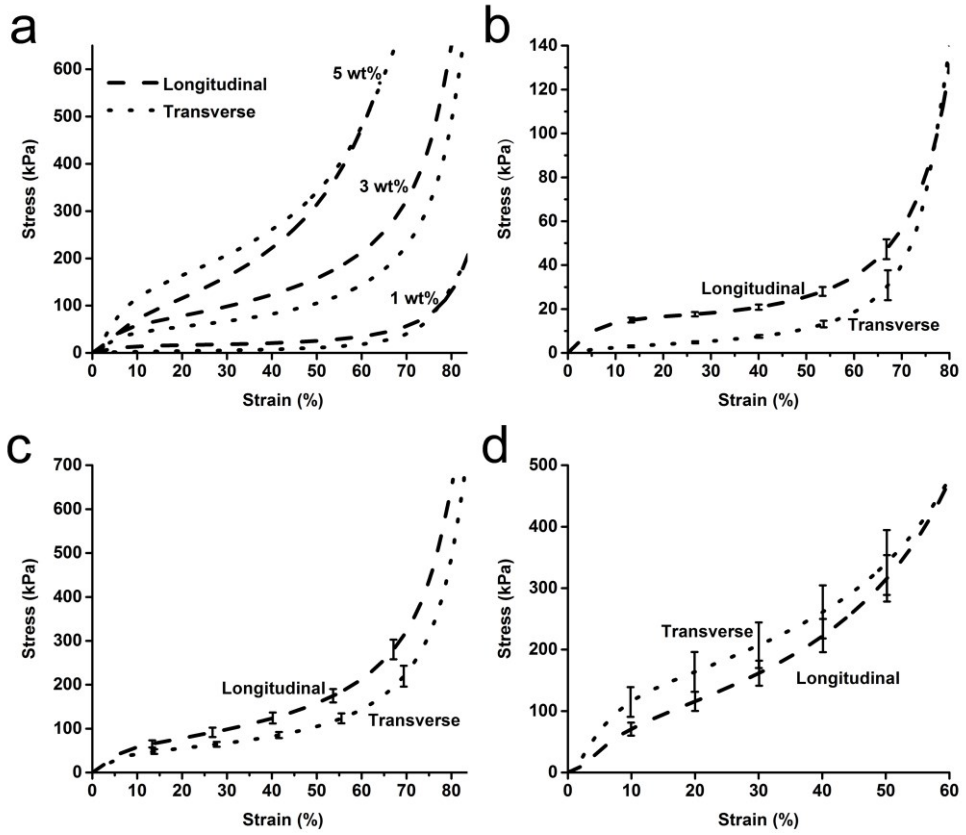

Fig. 6. (a) Comparing the compressive strength of the aerogels prepared from 1, 3 and 5 wt% CNF suspensions. Comparison of the longitudinal and transverse strength of the (b) 1 wt%, (c) 3 wt% and (d) 5 wt% aerogels.

The aerogels prepared from a 1 wt% CNF suspension were chosen to be used in the composite preparation. The pore structures were more clearly defined and better aligned in these samples. In addition, they did not seem to have as high degree of aggregation as the higher fiber content samples.

3.3 Composite morphology

The composition of the nanocomposite material appears to be homogenous as can be seen in the photograph showing neat bio-epoxy and CNF/epoxy composite specimens (Fig. 7 a). The used epoxy resin is highly transparent and the nanocomposite material preserves some of the transparency. The fiber mass fraction in the composite is 11.7 wt%, which is significantly higher than the 1.7 wt% reported by Zhai *et al.* for the

PVA/CNF aerogels filled with PDMS [17]. This can be explained by the high degree of sample compaction occurring during the vacuum infusion process, resulting in a decreased volume (93 % reduction, mostly in thickness) and an increased fiber content.

Most of the aerogel pores are completely filled with the resin as can be seen in the FE-SEM images showing fracture surfaces of the composite sample (Fig. 7 b, c). A longitudinal cross section reveals wall structures that are mostly horizontally oriented in the image and the spaces between the walls are filled with the polymer (Fig. 7 b). On the other hand, epoxy-filled tubular pores perpendicular to the image plane are seen in the image of a transverse cross section (Fig. 7 c). In Fig. 7 d, a 3D model based on micro-CT scanning is shown. In the bottom part, both the matrix (blue) and the fiber (white) phases can be seen, and on the top part, only the fiber phase is visible. The fibers have formed lamellar walls that are homogenously distributed throughout the volume of interest. The lamellae appear to be mostly vertically aligned, again an indication of a unidirectional orientation of the fiber structure of the composite.

The calculated fiber, matrix and void volume fractions in the composite are 8 %, 80 % and 12 %, respectively. The obtained void content value is relatively high but this can be at least partly explained by the presence of some incompletely impregnated areas in the composite. These areas could be observed by visual inspection as a white color on the otherwise translucent material. In addition, the manual composite volume measurement may have not been completely accurate, resulting in a higher volume than the actual value. The majority of the aerogel appeared to be properly filled and for these areas, the void fraction can be assumed to be lower than the value obtained for the whole nanocomposite sample. Only the parts with no visible voids were used in the dynamic mechanical analysis.

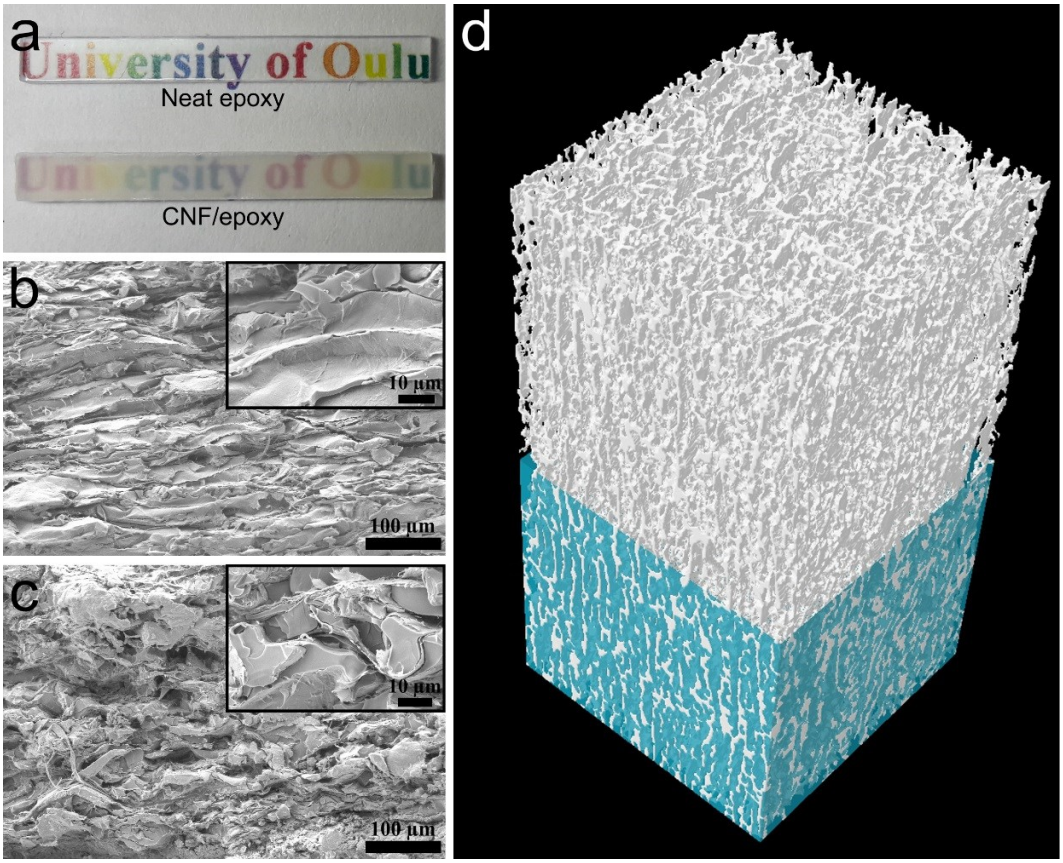

Fig. 7. Appearance and morphology of the composite sample. (a) A photograph of neat epoxy and composite specimens used in DMA testing (thickness varied between 1.0-1.4 mm), FE-SEM images of (b) vertical and (c) horizontal cross sections of the composite and (d) a 3D micro-CT model (240 x 240 x 480 μm^3 volume of interest) showing the matrix (blue) and fiber (white) phases.

3.4 Dynamic mechanical analysis

The results of the dynamic mechanical analysis (DMA) show significantly improved viscoelastic properties for the nanocomposites compared to the neat epoxy resin (Table 3, Fig. 8). The nanocomposite storage modulus (E') measured at 35 °C is 42-69 % higher than that of neat epoxy, depending on the testing direction. The nanofiber structure appears to be anisotropically oriented inside the polymer matrix as the storage modulus is higher in the longitudinal than in the transverse direction [21]. However, to

confirm the fiber orientation additional characterizations, such as X-ray scattering studies, should be conducted but were out of the scope of the current study.

The improvement in the storage modulus is even more remarkable at temperatures above the relaxation temperature. The neat bio-epoxy shows a rubbery behavior and loses its structural integrity, while the nanocomposite retains some of the stiffness in both directions. The E' of the epoxy sample at 100 °C is only 0.5 % of the E' at 35 °C. The nanocomposite in turn retains 5.5 and 13 % of its E' as measured in the transverse and longitudinal directions, respectively. This can most likely be ascribed to the properties of the hydrogen-bonded CNF network as similar findings have also been reported elsewhere [4,22]. The current results are lot more promising than those reported in a study by Barari *et al.* (2016), in which the storage modulus of the aerogel-based composites was worse than that of neat epoxy [18]. On the other hand, an over 170 % increase in Young's modulus has been reported for a CNF/PVA aerogel filled with a PDMS polymer, but because of the low fiber content and the poor properties of the polymer, the composite material was still very weak.

Table 3. Viscoelastic properties of the composite and the neat epoxy resin samples. The composite sample was tested in both the longitudinal (∥) and the transverse directions (⊥).

Sample	E' at 35 °C (MPa)	E' at 100 °C (MPa)	Tan δ peak (°C)
Neat epoxy	2620 (± 30)	14 (± 1)	59.6 (± 0.5)
Epoxy/CNF (⊥)	3710 (± 30)	203 (± 4)	62.1 (± 0.1)
Epoxy/CNF (∥)	4420 (± 120)	557 (± 45)	61.4 (± 0.1)

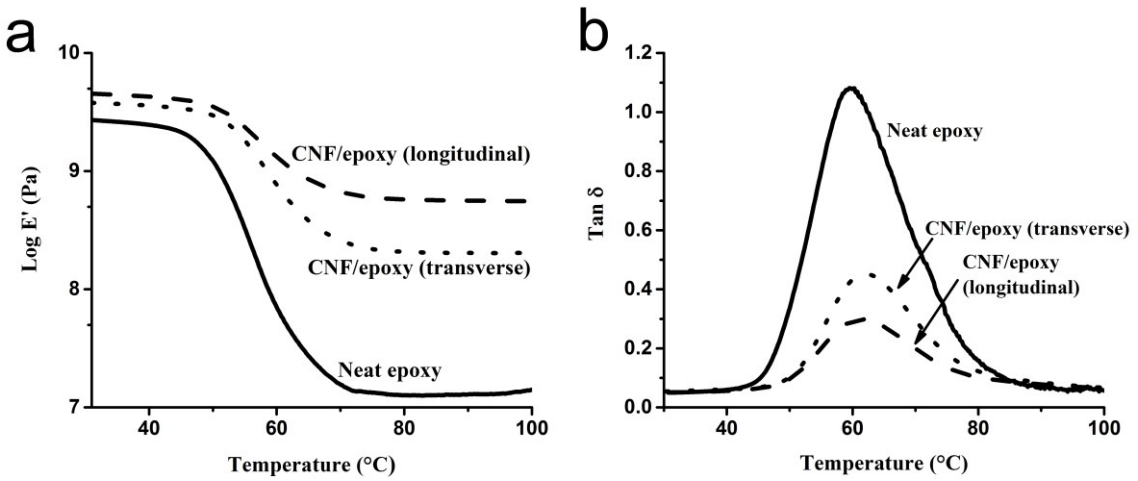

Fig. 8. Viscoelastic properties of the composite and the neat epoxy samples. (a) Storage modulus (E') and (b) tan δ as a function of temperature. The composite sample was tested in both the longitudinal and the transverse directions.

4 Conclusions

It was shown that freeze cast CNF aerogels can act as preforms in vacuum infusion. By filling them with a bio-epoxy resin, environmentally friendly and mechanically robust nanocomposites could be prepared. The impregnation time was significantly shorter than for the more commonly used paper-like CNF networks and the composite had an oriented CNF structure. This kind of preform material has a potential to be scaled up and utilized in commercial vacuum infusion processes to prepare composites that can be used for example in transportation applications. The low weight of the CNFs leads to weight reductions in the end products, thus decreasing the fuel consumption and reducing the greenhouse gas emissions.

To improve the process and to obtain composites with more homogenous and unidirectionally aligned fiber structures, the freezing temperature should be controlled throughout the freeze casting process. The means to achieve this already exist and are to be utilized in a future study. In addition, the mechanical properties of the composite

could be further improved either by increasing the aerogel density or by using compression moulding to obtain a more compacted material with a higher fiber content.

5 Acknowledgements

The authors acknowledge TEKES FiDiPro Programme, European Research Council under the European Union's Seventh Framework Programme (FP/2007-2013, ERC Grant Agreement no. 336267) and the Academy of Finland (grant no. 268378) for the financial support. The authors would also like to thank Shiyu Geng for performing the AFM imaging and Maiju Hietala for her help, especially in optical microscopy.

6 References

[1] I. Siró, D. Plackett, Microfibrillated cellulose and new nanocomposite materials: a review, Cellulose. 17 (2010) 459–494. doi:10.1007/s10570-010-9405-y.

[2] A.N. Nakagaito, H. Yano, Novel high-strength biocomposites based on microfibrillated cellulose having nano-order-unit web-like network structure, Appl. Phys. A. 80 (2005) 155–159. doi:10.1007/s00339-003-2225-2.

[3] M. Henriksson, L.A. Berglund, Structure and properties of cellulose nanocomposite films containing melamine formaldehyde, J. Appl. Polym. Sci. 106 (2007) 2817–2824. doi:10.1002/app.26946.

[4] M. Henriksson, L. Fogelström, L.A. Berglund, M. Johansson, A. Hult, Novel nanocomposite concept based on cross-linking of hyperbranched polymers in reactive cellulose nanopaper templates, Compos. Sci. Technol. 71 (2011) 13–17. doi:10.1016/j.compscitech.2010.09.006.

[5] M. Jonoobi, Y. Aitomäki, A.P. Mathew, K. Oksman, Thermoplastic polymer impregnation of cellulose nanofibre networks: Morphology, mechanical and

optical properties, Compos. Part Appl. Sci. Manuf. 58 (2014) 30–35. doi:10.1016/j.compositesa.2013.11.010.

[6] K.-Y. Lee, Y. Aitomäki, L.A. Berglund, K. Oksman, A. Bismarck, On the use of nanocellulose as reinforcement in polymer matrix composites, Compos. Sci. Technol. 105 (2014) 15–27. doi:10.1016/j.compscitech.2014.08.032.

[7] H. Sehaqui, N. Ezekiel Mushi, S. Morimune, M. Salajkova, T. Nishino, L.A. Berglund, Cellulose Nanofiber Orientation in Nanopaper and Nanocomposites by Cold Drawing, ACS Appl. Mater. Interfaces. 4 (2012) 1043–1049. doi:10.1021/am2016766.

[8] C. Baez, J. Considine, R. Rowlands, Influence of drying restraint on physical and mechanical properties of nanofibrillated cellulose films, Cellulose. 21 (2014) 347–356.

[9] S. Hooshmand, Y. Aitomäki, N. Norberg, A.P. Mathew, K. Oksman, Dry-Spun Single-Filament Fibers Comprising Solely Cellulose Nanofibers from Bioresidue, ACS Appl. Mater. Interfaces. 7 (2015) 13022–13028. doi:10.1021/acsami.5b03091.

[10] S. Hooshmand, Y. Aitomäki, L. Berglund, A.P. Mathew, K. Oksman, Enhanced alignment and mechanical properties through the use of hydroxyethyl cellulose in solvent-free native cellulose spun filaments, Compos. Sci. Technol. 150 (2017) 79–86. doi:10.1016/j.compscitech.2017.07.011.

[11] S. Iwamoto, A. Isogai, T. Iwata, Structure and Mechanical Properties of Wet-Spun Fibers Made from Natural Cellulose Nanofibers, Biomacromolecules. 12 (2011) 831–836. doi:10.1021/bm101510r.

[12] A. Walther, J.V.I. Timonen, I. Díez, A. Laukkanen, O. Ikkala, Multifunctional High-Performance Biofibers Based on Wet-Extrusion of Renewable Native Cellulose Nanofibrils, Adv. Mater. 23 (2011) 2924–2928. doi:10.1002/adma.201100580.

[13] K.M.O. Håkansson, A.B. Fall, F. Lundell, S. Yu, C. Krywka, S.V. Roth, G. Santoro, M. Kvick, L. Prahl Wittberg, L. Wågberg, L.D. Söderberg, Hydrodynamic alignment and assembly of nanofibrils resulting in strong cellulose filaments, Nat. Commun. 5 (2014). doi:10.1038/ncomms5018.

[14] J. Lee, Y. Deng, The morphology and mechanical properties of layer structured cellulose microfibril foams from ice-templating methods, Soft Matter. 7 (2011) 6034. doi:10.1039/c1sm05388d.

[15] P. Munier, K. Gordeyeva, L. Bergström, A.B. Fall, Directional Freezing of Nanocellulose Dispersions Aligns the Rod-Like Particles and Produces Low-Density and Robust Particle Networks, Biomacromolecules. 17 (2016) 1875–1881. doi:10.1021/acs.biomac.6b00304.

[16] Z.-Z. Pan, H. Nishihara, S. Iwamura, T. Sekiguchi, A. Sato, A. Isogai, F. Kang, T. Kyotani, Q.-H. Yang, Cellulose Nanofiber as a Distinct Structure-Directing Agent for Xylem-like Microhoneycomb Monoliths by Unidirectional Freeze-Drying, ACS Nano. 10 (2016) 10689–10697. doi:10.1021/acsnano.6b05808.

[17] T. Zhai, Q. Zheng, Z. Cai, L.-S. Turng, H. Xia, S. Gong, Poly(vinyl alcohol)/Cellulose Nanofibril Hybrid Aerogels with an Aligned Microtubular Porous Structure and Their Composites with Polydimethylsiloxane, ACS Appl. Mater. Interfaces. 7 (2015) 7436–7444. doi:10.1021/acsami.5b01679.

[18] B. Barari, T.K. Ellingham, I.I. Ghamhia, K.M. Pillai, R. El-Hajjar, L.-S. Turng, R. Sabo, Mechanical characterization of scalable cellulose nano-fiber based composites made using liquid composite molding process, Compos. Part B Eng. 84 (2016) 277–284. doi:10.1016/j.compositesb.2015.08.040.

[19] S. Deville, E. Saiz, A.P. Tomsia, Ice-templated porous alumina structures, Acta Mater. 55 (2007) 1965–1974. doi:10.1016/j.actamat.2006.11.003.

[20] T. Waschkies, R. Oberacker, M.J. Hoffmann, Investigation of structure formation during freeze-casting from very slow to very fast solidification velocities, Acta Mater. 59 (2011) 5135–5145. doi:10.1016/j.actamat.2011.04.046.

[21] I. Kvien, K. Oksman, Orientation of cellulose nanowhiskers in polyvinyl alcohol, Appl. Phys. A. 87 (2007) 641–643. doi:10.1007/s00339-007-3882-3.

[22] F. Ansari, S. Galland, M. Johansson, C.J.G. Plummer, L.A. Berglund, Cellulose nanofiber network for moisture stable, strong and ductile biocomposites and increased epoxy curing rate, Compos. Part Appl. Sci. Manuf. 63 (2014) 35–44. doi:10.1016/j.compositesa.2014.03.017.

Figure captions

Fig. 1. CNF morphology. AFM (a) height and (b) phase images and (c) an optical microscope image showing the various fiber sizes present in the material.

Fig. 2. The vacuum infusion process. (a) A schematic illustration and (b) a photograph of the used vacuum infusion setup.

Fig. 3. Photographs of aerogels. (a) Three differently shaped samples (in all of the samples the freezing direction is from bottom up), (b) a sample supporting ~400 times its weight and a sample (c) being bent and (d) after bending.

Fig. 4. Microstructure of the CNF aerogels. FE-SEM images of fractured vertical cross sections of the (a) bottom, (b) middle and (c) top parts of an ~65 mm high 1 wt% sample, and of middle parts of ~9 mm high (d) 1 wt%, (e) 3 wt% and (f) 5 wt% samples.

Fig. 5. Images of 3D micro-CT reconstructions of the aerogels. (a-c) Vertical and (d-f) horizontal cross-sections of 1 wt% (a, d), 3 wt% (b, e) and 5 wt% (c, f) aerogels.

Fig. 6. (a) Comparing the compressive strength of the aerogels prepared from 1, 3 and 5 wt% CNF suspensions. Comparison of the longitudinal and transverse strength of the (b) 1 wt%, (c) 3 wt% and (d) 5 wt% aerogels.

Fig. 7. Appearance and morphology of the composite sample. (a) A photograph of neat epoxy and composite specimens used in DMA testing (thickness varied between 1.0-1.4 mm), FE-SEM images of (b) vertical and (c) horizontal cross sections of the composite and (d) a 3D micro-CT model (240 x 240 x 480 μm^3 volume of interest) showing the matrix (blue) and fiber (white) phases.

Fig. 8. Viscoelastic properties of the composite and the neat epoxy samples. (a) Storage modulus (E') and (b) tan δ as a function of temperature. The composite sample was tested in both the longitudinal and the transverse directions.

Table captions

Table 1. Density, porosity and BET specific surface area of the prepared aerogels.

Table 2. Aerogel compressive strengths. The testing was conducted in both the longitudinal (∥) and the transverse (⊥) directions.

Table 3. Viscoelastic properties of the composite and the neat epoxy resin samples. The composite sample was tested in both the longitudinal (∥) and the transverse directions (⊥).